Withaferin A induces heme oxygenase (HO-1) expression in endothelial cells via activation of the Keap1/Nrf2 pathway

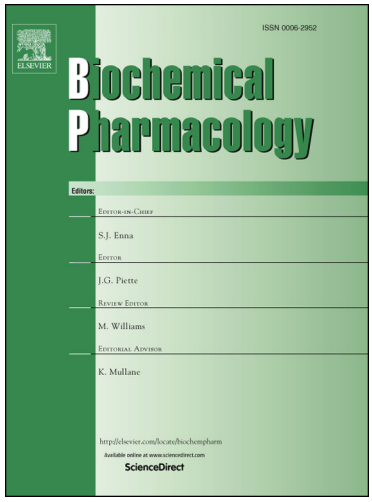

Withaferin A induces heme oxygenase (HO-1) expression in endothelial cells via activation of the Keap1/Nrf2 pathway

Karen Heyninck, Linde Sabbe, Chandra Sekhar Chirumamilla, Katarzyna Szarc vel Szic, Pieter Vander Veken, Kristien J.A. Lemmens, Maija Lahtela-Kakkonen, Stefan Naulaerts, Ken Op de Beeck, Kris Laukens, Guy Van Camp, Antje R. Weseler, Aalt Bast, Guido R.M.M. Haenen, Guy Haegeman, Wim Vanden Berghe

PII: S0006-2952(16)30022-3
DOI: http://dx.doi.org/10.1016/j.bcp.2016.03.026
Reference: BCP 12526

To appear in: *Biochemical Pharmacology*

Received Date: 11 January 2016
Accepted Date: 31 March 2016

Please cite this article as: K. Heyninck, L. Sabbe, C.S. Chirumamilla, K.S.v. Szic, P.V. Veken, K.J.A. Lemmens, M. Lahtela-Kakkonen, S. Naulaerts, K. Op de Beeck, K. Laukens, G. Van Camp, A.R. Weseler, A. Bast, G.R.M. Haenen, G. Haegeman, W.V. Berghe, Withaferin A induces heme oxygenase (HO-1) expression in endothelial cells via activation of the Keap1/Nrf2 pathway, *Biochemical Pharmacology* (2016), doi: http://dx.doi.org/10.1016/j.bcp.2016.03.026

Withaferin A induces heme oxygenase (HO-1) expression in endothelial cells via activation of the Keap1/Nrf2 pathway

Karen Heyninck[1,*,#], Linde Sabbe[1,*], Chandra Sekhar Chirumamilla[2], Katarzyna Szarc vel Szic[2], Pieter Vander Veken[3], Kristien J.A.Lemmens[4], Maija Lahtela-Kakkonen[5], Stefan Naulaerts[6,7], Ken Op de Beeck[8,9], Kris Laukens[6,7], Guy Van Camp[9], Antje R. Weseler[4], Aalt Bast[4], Guido R.M.M. Haenen[4], Guy Haegeman[1], Wim Vanden Berghe[1,2]

[1] Laboratory of Eukaryotic Gene Expression and Signal Transduction (LEGEST), Department of Biochemistry and Microbiology, Ghent University, Proeftuinstraat 86, Gent, Belgium

[2] Laboratory of Protein Science, Proteomics and Epigenetic Signaling (PPES), Department of Biomedical Sciences, University of Antwerp, Campus Drie Eiken, Universiteitsplein 1, Wilrijk, Belgium

[3] Laboratory of Medicinal Chemistry, University of Antwerp, Campus Drie Eiken, Universiteitsplein 1, Wilrijk, Belgium

[4] Department of Pharmacology and Toxicology, Maastricht University, Universiteitssingel 50, 6229ER Maastricht, The Netherlands

[5] School of Pharmacy, Pharmaceutical Chemistry, University of Eastern Finland, 70211 Kuopio, Finland.

[6] Biomedical Informatics Research Center Antwerp (Biomina), University of Antwerp & University Hospital Antwerp, Campus Middelheim, Middelheimlaan 1, Antwerpen, Belgium

[7] Advanced Database Research and Modelling (ADReM), Department of Mathematics & Computer sciences, University of Antwerp (UA), Campus Middelheim, Middelheimlaan 1, Antwerpen, Belgium.

[8]Center of Medical Genetics, Department of Biomedical Sciences, University of Antwerp, Campus Drie Eiken, Universiteitsplein 1, Wilrijk, Belgium

[9] Center for Oncological Research (CORE) Antwerp, Laboratory of Cancer Research and Clinical Oncology, University of Antwerp, Universiteitsplein1, Wilrijk, Belgium.

[*] KH and LS contributed equally to this work

[#] To whom correspondence should be addressed: Karen Heyninck, Laboratory of Eukaryotic Gene Expression and Signal Transduction (LEGEST), Department of Biochemistry and Microbiology, Ghent University, Proeftuinstraat 86, 9000 Gent, Belgium, Tel.: +(32)92645147; Fax: +(32)92645304; E-mail: karen.heyninck@ugent.be

Keywords: antioxidant, endothelial cell, molecular pharmacology, phytochemical, signal transduction, transcription regulation

ABSTRACT

Withaferin A (WA), a natural phytochemical derived from the plant W*ithania somnifera,* is a well-studied bioactive compound exerting a broad spectrum of health promoting effects. To gain better insight in the potential therapeutic capacity of WA, we evaluated the transcriptional effects of WA on primary human umbilical vein endothelial cells (HUVECs) and an endothelial cell line (EA.hy926). RNA microarray analysis of WA treated HUVEC cells demonstrated increased expression of the antioxidant gene heme oxygenase (HO-1). Transcriptional regulation of this gene is strongly dependent on the transcription factor NF-E2-related factor 2 (Nrf2), which senses chemical changes in the cell and coordinates transcriptional responses to maintain chemical homeostasis via expression of antioxidant genes and cytoprotective Phase II detoxifying enzymes. Under normal conditions, Nrf2 is kept in the cytoplasm by Kelch-like ECH-associated protein 1 (Keap1), an adaptor protein controlling the half-life of Nrf2 via constant proteasomal degradation. In this study we demonstrate that WA time- and concentration-dependently induces HO-1 expression in endothelial cells via upregulation and increased nuclear translocation of Nrf2. According to the crucial negative regulatory role of Keap1 in Nrf2 expression levels, a direct interaction of WA with Keap1 could be demonstrated. *In vitro* and *in silico* evaluations suggest that specific cysteine residues in Keap1 might be involved in the interaction with WA.

1. Introduction

The plant *Withania somnifera*, also known as “Ashwagandha”, “Indian ginseng” or “winter cherry”, is popular in Ayurvedic medicine, an ancient medicinal system of Indian origin based on the therapeutic use of herbs and natural products. Various extract preparations have been used to treat a wide range of disorders like chronic fatigue, dehydration or rheumatism for over thousands of years. The main bio-active chemical constituents of *Withania somnifera* are the withanolides, a class of chemicals containing a steroidal alkaloid and a lactone structure. From these various withanolides, Withaferin A (WA), a highly oxygenated withanolide, is by far the most studied bioactive compound. Chemical structure analysis of WA pinpointed 3 positions that could be involved in an alkylation reaction with nucleophilic sites like sulfhydryl groups of cysteine residues in target proteins. These positions are the epoxide structure at C5 and an unsaturated ketone at C3 and C24, being all highly susceptible for nucleophilic attack to target proteins, resulting in a covalent binding via a Michael addition alkylation reaction [1]. WA was demonstrated to exert a broad spectrum of health promoting effects including anti-inflammatory, anti-carcinogenic, anti-angiogenic and pro-apoptotic properties. Despite this wide variety of therapeutic capacities of the compound, the molecular mechanisms underlying these activities remain largely unknown.

Nonetheless certain proteins have already been identified as targets of WA, including the intermediate filament proteins vimentin, glial fibrillary acidic protein and desmin, chaperones such as hsp90 and various kinases (reviewed in [2]). By these interactions, WA was shown to regulate several signal transduction cascades involved in cell death, inflammatory responses, proliferation, metastasis and transcriptional regulation. In case of its regulatory role on transcriptional processes, positive and negative effects have been described, including inhibition of transcription mediated by NF-κB, Notch-1, STAT1 and STAT3, and activation of transcription mediated by heat shock factor-1 and LXRα [1, 3-8]. Besides these *in vitro* and *in vivo* studies, *in silico* molecular docking studies revealed the possibility of strong intermolecular interactions of WA with some crucial intracellular mediators of different signal transduction pathways, including the hsp90-binding protein CDC37, the adaptor protein IKKγ involved in NF-κB activation, the tumor suppressor protein p53, the cell cycle regulating protein p21, and the stress chaperone mortalin [9-13]. In the latter study a potential binding of WA to the transcription factor NF-E2 related factor 2 (Nrf2) was also suggested. Nrf2 is a cap´n´collar basic leucine zipper transcription factor belonging to a group of xenobiotic- and oxidative stress-activated receptors. Nrf2 senses chemical changes in the cell and coordinates transcriptional responses to maintain the chemical homeostasis of the cell via the expression of a battery of more than 200 genes including antioxidant genes and other cytoprotective Phase II detoxifying enzymes via the presence of an antioxidant

response element (ARE)/electrophile response element (EpRE) in their promoter region [14]. Among these Nrf2-regulated genes, heme oxygenase-1 (HO-1) is one of the most studied examples.

In inactivated cells, Nrf2 is associated in the cytoplasm with the Kelch-like ECH-associated protein 1 (Keap1) [15]. This BTB and Kelch domain containing protein is an adaptor, which bridges Nrf2 to Cullin3 (Cul3)-based E3 ligase thereby regulating the stability of Nrf2 via constitutive ubiquitination and proteasomal degradation [16-18]. Under quiescent conditions, Nrf2 is constantly degraded having a half-life of less than 20 minutes [19]. Keap1 is a thiol-rich protein that has multiple reactive cysteines required for activation of Nrf2. Several electrophilic reagents have been shown to directly target these cysteine residues (reviewed in [20]). Using transgenic complementation rescue analysis in mice mainly 3 cysteine residues, i.e. C151, C273 and C288, have been demonstrated to be indispensable for Keap1 mediated ubiquitination of Nrf2 [21]. Modifications of these cysteines in Keap1 lead to conformational changes in the Nrf2-Keap1-Cul3 complex whereby Nrf2 can no longer be ubiquitinated and escapes from subsequent degradation. Thereby accumulation of the transcription factor occurs, leading to its nuclear translocation, heterodimer formation with small MAF proteins and increased transcription of Nrf2 target genes [22].

To gain better insight in the potential therapeutic properties of WA, we investigated the effects of WA on transcriptional processes in vascular endothelial cells. This analysis supported strong evidence for WA-mediated activation of the transcription factor Nrf2. In primary endothelial cells as well as in an endothelial cell line, we further investigated how WA activates Nrf2 signaling. By means of biotinylated WA and pull-down experiments, the possible electrophilic interactions of WA with Keap1 was evaluated. Finally, *in silico* docking modeling and proteomic analysis of WA-modified Keap1 has been applied to identify cysteine residues which may react with WA through a covalent Michael addition reaction.

2. Materials and methods

2.1 Materials

Withaferin A (WA) and Withanone (WN) were purchased from ChromaDex (Santa Ana, CA). Both compounds were solubilized in DMSO at 20mM. MG-132 and cycloheximide (CHX) were obtained from Sigma (St. Louis, MO). Anti-Nrf2 and anti-FLAG tag antibody were purchased from Abcam (Cambridge, UK), anti-HO-1 from Gentaur (Kampenhout, BE), anti-Keap1 from Bio-Connect (TE Huissen, NL), anti-Keap1N from Santa Cruz Biotechnology (Santa Cruz, CA), anti-ubiquitin from Cell Signaling Technology (Danvers, MA), anti-HA clone 16B12 from Covance Research Products (Berkeley, CA), anti-tubulin and anti-FLAG M2 affinity gel from Sigma (St. Louis, MO), and IRdye coupled secondary antibodies (Rockland, Gilbertsville, PA). siRNA Nrf2 plus SMART pool (L-003755-00-0005) and non-targeting pool (D-001810-10-05) were obtained from Dharmacon (Lafayette, CO). Neutravidin agarose beads were purchased from Thermo Scientific (Rockford, IL), Protein A on Trisacryl beads from Pierce Protein Biology (Rockford, IL). Recombinant Keap1-protein was obtained from Sino Biological (Beijing, China). Trypsin was purchased from Promega (Madison, USA). Ammonium bicarbonate (ABC) acetonitrile (ACN), α-cyano-4-hydroxycinnamic acid and trifluoroacetic acid (TFA) were acquired from Sigma (St. Louis, MO).

2.2 Cell culture

The EA.hy926 cell line was a kind gift of Dr. Voets (Catholic University Leuven, Department of Cell and Molecular Medicine, Laboratory of Ion Channel Research, BE). This hybridoma of the human umbilical vein endothelial cell (HUVEC) with the human epithelial cell line A549 has been shown to retain several native endothelial cell properties [23]. Cells were cultured in Dulbecco´s Modified Eagle´s Medium supplemented with 10% fetal bovine serum, 100 U/ml penicillin, 100µg/ml streptomycin and HAT selection supplement (Invitrogen, Carlsbad, CA) in mycoplasma- and endotoxin-free conditions. Primary HUVEC cells were cultured in EBM Basal Phenol Red Free medium supplemented with EGM SingleQuot Kit containing supplements and growth factors (Lonza, CH). All HUVEC cells were used in experiments at the third passage level. Human embryonic kidney HEK293T cells were used in cellular assays requiring high transfection efficiencies. These cells were a kind gift of Dr. M. Hall (University of Birmingham, UK). Cells were grown in Dulbecco's modified Eagle's medium supplemented with 10% fetal bovine serum, 2 mM L-glutamine, 0.4 mM sodium pyruvate and penicillin/streptomycin.

2.3 Plasmids

Eukaryotic expression pCDNA3 plasmids encoding Keap1 or its deletion mutants, Keap1-ΔBTB, Keap1-Δlink and Keap1-ΔKelch, as well as pGL4.22-hNQO1-ARE-luc, a luciferase reporter plasmid with ARE binding site of human NQO1 gene, were generously provided by. Dr. D.D. Zhang (University of Arizona, Tucson, AZ). The eukaryotic expression vector pUT651 encoding β-galactosidase was obtained from Eurogentec.

2.4 MTT cell viability assay

Cells seeded in 96-well plates were treated with various concentrations of WA, WA-BIOT or WN. After 24 hours incubation, 10µl MTT reagent was added to each well and incubated for an additional 4 hours. Solubilization of the formed MTT crystals was achieved by addition of 40µl of SDS/HCl solution per well. Plates were incubated overnight at room temperature. Absorbance was measured at 595 nm using a plate reader (Victor 3 Wallac 1420, Perkin Elmer Life Sciences).

2.5 mRNA microarray processing and data analysis

Following trizol extraction from HUVEC cells which were left untreated or exposed for 6 h to 1 µM WA in 3 independent experiments, RNA was quality controlled on a Bio-Rad experion (Bio-Rad, Hercules, CA, USA). Samples with 28S/18S rRNA ratio > 1.8 and A260/A280 ratio between 1.9-2.1 were used for further analysis. 500ng of total RNA was amplified using the Illumina TotalPrep RNA Amplification kit (Life Technologies, Carlsbad, CA, USA). RNA was reverse transcribed using T7 oligo(dT) primers after which biotinylated cRNA was synthesized through *in vitro* transcription reaction. 750ng of amplified cRNA was hybridized to a corresponding array of a HumanHT12 bead chip (Illumina, San Diego, CA). The bead chip was incubated for 18 hours at 58°C in a hybridization oven whilst continuous rocking. After several consecutive washing steps, bead intensities were read on Illumina iScan. Raw data intensities were read in R using the "bead array" package (v2.8.1) [24]. Intensities were normalized and differential gene expression between samples was estimated using "limma" (v3.14.1) [25]. Resulting p-values were corrected for multiple hypothesis testing using the Benjamini-Hochberg procedure. Next to estimating gene expressions, euclidean distances between samples were calculated and used as a distance metric in a hierarchical cluster analysis. Transcriptomic analysis was done by uploading Illumina bead array gene expression data into Ingenuity Pathway Analysis software (IPA) and performing a core analysis. Each identifier was mapped to its corresponding gene object in the Ingenuity knowledge base. A fold change cut-off of 2 as well as false discovery rate of 0.05% were set to identify genes whose expression was significantly differentially regulated. These genes, called focus genes, were overlaid onto a global molecular network developed from information contained in the Ingenuity knowledge base. Networks of these focus genes were

then algorithmically generated based on their connectivity. The Bio Functional Analysis identified the biological functions and/or diseases that were most significant to the data set. Genes from the dataset that met the abovementioned cut-off and were associated with biological functions and/or diseases in the Ingenuity knowledge base were considered for the analysis. Fisher's exact test was used to calculate a p-value determining the probability that each biological function and/or disease assigned to that data set is due to chance alone. This mRNA microarray processing and hierarchical clustering was performed by the Department of Biomedical Sciences, in Human Molecular Genetics Group of Dr. Van Camp.

2.6 RNA isolation and qPCR

Cells, seeded in 6-well plates, were stimulated for 6 hours with various concentrations of WA or with 1µM WA at several time points. As a control cells were treated with DMSO for 6 hours. After incubation total RNA was extracted by the acid-guanidinium-thiocyanate-phenol chloroform method using Trizol Reagent (Invitrogen, Carlsbad, CA). 0.5µg of total RNA was used to perform reverse transcription using MMLV reverse transcriptase (Promega, Madison, WI). Real-time polymerase chain reaction (qPCR) was performed on the Light Cycler 480II system (Roche, Basel, CH) using the SYBR green Master Mix (Biorad, Hercules, CA) and the following gene specific primer sets: HMOX1 fwd 5'-CCAGCGGGCCAGCAACAAAGTGC-3' and HMOX1 rev 5'-AAGCCTTCAGTGCCCACGGTAAGG-3', PPIA fwd 5'-GCATACGGGTCCTGGCATCTTGTCC-3' and PPIA rev 5'-ATGGTGATCTTCTTGCTGGTCTTGC-3', GAPDH fwd 5'-GCTCTGCTCCTCCTGTTC-3' and GAPDH rev 5'-ACGACCAAATCCGTTGACTC-3', Nrf2 fwd 5'-TTCCCGGTCACATCGAGAG-3' and Nrf2 rev 5'-TCCTGTTGCATACCGTCTAAATC-3'. Primers used for qPCR validation of the mRNA array data were produced by Qiagen (HSPB8 PPH11188B-200; DNAJB9 PPH05919A-200; HERPUD1 PPH126061-200; GCLM PPH02099A-200; SQSTM1 PPH02107A-200; ENC1 PPH00878A-200). Efficiency and relative mRNA amounts were calculated for every run by the use of a standard curve. Relative mRNA values were normalized to GAPDH as a reference gene.

2.7 Western immunoblotting

Cells were left untreated or were treated with different doses of WA, WN or DMSO, and MG132 or CHX for different time points. At the end of the incubation time, whole cell lysates were prepared in SDS sample buffer (62.5mM Tris–HCl pH6.8, 2% SDS, 10% glycerol, 0.5% DTT). Proteins were separated by loading equal amounts of the lysates on a 8.5% SDS-PAGE and presence of the proteins of interest was evaluated via western blotting using specific HO-1, Nrf2, Keap1, HA, FLAG or tubulin recognizing primary antibodies and visualized by fluorophore-coupled secondary antibodies. Tubulin was used as a loading

control protein. Detection was performed by use of the Odyssey Imaging System (Licor, Lincoln, NA) and quantification of the bands was performed using the Odyssey Imaging System software.

2.8 siRNA silencing

Cells were transfected with 25nM siRNA Nrf2 siGENOME plus SMART pool via the Dharmafect transfection reagent number 1 following the protocol as described by Thermo Scientific. A non-targeting pool was used as a negative control to assess a-specific effects. 24 hours after transfection cells were induced with WA for the indicated time periods. Subsequently, cells were lysed in SDS sample buffer or RNA was isolated, as described above.

2.9 Nuclear and cytoplasmic extraction

Cells were stimulated with 1µM WA for several time points before lysis in B1 buffer (10mM HEPES pH7.5, 10mM KCl, 1mM $MgCl_2$, 5% glycerol, 0.5mM EDTA pH 7.5, 0.1mM EGTA pH 7.5, 0.5mM DTT, protease inhibitors and 0.65% NP-40). Nuclei were pelleted by centrifugation at 800 rpm for 15 minutes and lysed in B2 buffer by shaking 15 minutes at 4°C (20mM HEPES pH7.5, 1% NP-40, 1mM $MgCl_2$, 400mM NaCl, 10mM KCl, 20% glycerol, 0.5mM EDTA pH7.5, 0.1mM EGTA pH7.5, 0.5mM DTT and protease inhibitors). Concentrations of protein samples were measured using the Pierce BCA protein assay kit (Thermo Scientific, Rockford, IL) and equal protein amounts were subsequently analyzed by western blotting for detection of the protein of interest. In these assays tubulin and PARP detection were added as loading control and to validate fractionation, being respectively a cytoplasmic and nuclear marker.

2.10 ARE-dependent luciferase reporter assay

HEK293T cells were seeded in 24-well plates and transiently transfected by a standard PEI co-precipitation method using 200 ng DNA per well. Each transfection setup contained 80 ng empty vector, 80 ng of pGL4-hNQO1-ARE-luc plasmid and 40 ng pUT651 plasmid. Twenty-four hours after transfection, cells were left untreated or were treated with 1 or 2 µM WA, or corresponding concentration of DMSO, as indicated. After 24 hours incubation, cells were lysed in 100 µl lysis buffer and ARE-dependent luciferase activity was measured by using the Firefly Luciferase Glow Assay Kit (Pierce, Rockford, IL). Also activity of constitutively expressed β-galactosidase was measured by using Galacto-Star -Galactosidase Reporter Gene Assay System (Applied Biosystems, Bedford, MA) to normalize for differences in transfection efficiency.

2.11 Ubiquitination assay

HEK293T cells were transiently transfected using PEI transfection procedure with expression vectors encoding HA-tagged NRF2, FLAG-tagged NRF2 and Keap1. 24 hours after transfection cells were left untreated or were treated with WA for 2h and with MG132 for 1,5h to stabilize NRF2 expression. Cells were lysed in lysis buffer (5mM Tris-HCl pH7.5, 1% Triton-X100, 5mM EDTA, with the phosphatase and protease inhibitors NaF, aprotinin, pefabloc and leupeptin) supplemented with 2% SDS. Samples were boiled for 10 minutes at 95°C to disrupt protein-protein interactions while keeping the ubiquitination profile intact. Samples were diluted with lysis buffer without SDS to a final SDS concentration of 0,4%. Immunoprecipitation of NRF2 was performed using anti-NRF2 antibodies and protein A on Trisacryl beads. Samples were analyzed by western blot and evaluated for the expression of NRF2, Keap1 and ubiquitination of NRF2 using specific antibodies.

2.12 Affinity binding study

To analyze the interaction of WA with endogenous Keap1, Ea.hy926 cells were incubated for 2 hours with 1µM biotinylated WA (WA-BIOT) or 1µM biotin. Additionally, pre-incubation for 1 hour with 1 µM WA and co-incubation with 1µM DTT were evaluated. After incubation cells were lysed in buffer A (5mM Tris-HCl pH7.5, 1% Triton-X100, 5mM EDTA, supplemented with the phosphatase and protease inhibitors NaF, aprotinin, pefabloc and leupeptin). Proteins present in the soluble supernatant fractions were evaluated by western blotting. Pull down of WA interacting proteins from these samples was performed by addition of neutravidin beads and rotation of the samples overnight at 4°C. Beads were washed 5 times in lysis buffer and proteins were eluted from the beads by addition of 2x SDS sample buffer and boiling the samples. Subsequently, samples containing WA interacting proteins were analyzed by western blotting.

To define the interaction domain in Keap1 involved in the binding of WA, HEK293T cells were transiently transfected with WT or deletion mutant encoding eukaryotic expression vectors via standard PEI transfection procedure. 24 hours later, transfected cells were incubated with 1uM WA-BIOT or 1µM biotin for 2 hours. Samples were further processed as described above.

2.13 Adduct identification

Keap1 was incubated with 50µM WA or 50µM WN in 50mM ABC buffer pH7.4 for 30 min at 37°C. Keap1 (0.1mg/ml) was digested by trypsin during 2 hours at 37°C. The digested samples were diluted 1:10 in TFA. After dilution, 1µl of the digest and 1µl of matrix solution (2.5mg/ml α-cyano-4-hydroxycinnamic acid in 50% ACN/0.1% TFA) was spotted on a 348-well-format target plate and air-dried. Mass spectra were measured on the MALDI-TOF/TOF mass spectrometer (4800 MALDI-TOF/TOF analyzer; Applied Biosystems).

2.14 Covalent docking of WA with human Keap1

The keap1 protein of *H. sapiens* contains 624 amino acids containing 2 main structural domains: the BTB domain (67-179) and KELCH 1-6 domains (327-611). Due to the availability of crystal structures of only certain regions of KEAP1 in protein data bank, we have used 2.35 Å resolution crystal structure of BTB domain (PDB id: 4CXI) for covalent docking of WA to Cys151 and 1.8 Å resolution crystal structure of KELCH domain (PDB id: 4IFL) for covalent docking of WA to Cys489 and Cys434. Because a complete crystal structure of Keap1 is not yet available, we performed covalent docking of WA to Cys319, and Cys613 on a human Keap1 homology model built by the I-TASSER algorithm (http://zhanglab.ccmb.med.umich.edu/I-TASSER/) by combining crystal structures of Keap1 (1U6DX [26], 2DYHA [27], 3HVEA [28], 3I3NA (Murray, unpublished), 3ZGD [29], 4AP2A [30], and 4IFJ (Pan, unpublished)). The overall quality and pattern of non-bonded atomic interactions of homology built Keap1 model was verified by ERRAT. (http://services.mbi.ucla.edu/ERRAT/). Before proceeding to the covalent docking homology models with WA, the homology built full length Keap1 protein structure is energy minimized by the YASARA force field algorithm, by calculating corresponding hydrophobic side chains of a PDB converted into qualitative energies [31] (http://www.yasara.org/minimizationserver.htm). Cloud computing was applied to calculate covalent docking scores towards the specified cysteines [32]. Covalent docking is based on the Autodock source code 4.2 compatible with the existing scoring function of docking and molecular geometry constrains of the covalent linkages [33]. To ensure the optimal geometry of the bound ligand during the covalent docking, the structural changes of ligand were restricted to minimize variation in chiral WA conformations. The binding site was defined by selecting SH groups of specific cysteines. The docking solutions were evaluated based on their scoring function and the generated poses were clustered based on the cluster ranks of ligands. At the end of the docking procedure clusters were differentiated based on the covalent bond lengths and the docking score.

3. Results

3.1 Transcriptome profiling and pathway analysis of Withaferin A treated HUVEC cells

During recent years, evidence steadily increases that many therapeutic phytochemicals do not target single proteins but rather protein networks or pathways. To characterize pathways affected by WA in HUVEC cells, Illumina mRNA array analysis was performed to define WA responsive gene clusters. Therefore HUVEC cells were left either untreated or were treated with 1 µM WA for 6 hours. To reduce noisiness of the data, both setups were performed as biological triplicates. Identification of the statistically most important differentially expressed genes in the two conditions tested, WA treated vs. untreated, was obtained by delineating the log ratio cut off at 1 and the false discovery rate at 0.05%. Significance values were calculated via the Fisher's exact test to select specifically significant changes in the expression of every gene among repeated measurements. Biological interpretation of transcriptomic changes was done by uploading gene expression datasets into IPA software and performing core analysis.

In the microarray, about 48000 mRNAs were evaluated for expression changes in untreated and WA-treated HUVEC cells. Applying the threshold conditions, only 53 genes (about 0,11%) were detected as being significantly differentially expressed. These included 45 genes being upregulated by WA and 8 genes down-regulated by WA (Table 1).

To interpret the gene expression data in the context of biological processes and pathways, which might be altered in response to WA, IPA core analysis was applied to determine overrepresented signaling and metabolic canonical pathways. Although the gene set of differentially expressed genes was rather limited, this analysis method identified significantly overrepresented molecular pathways in the imported data set. Among them the Nrf2-mediated oxidative stress response pathway was shown to be the most significantly impacted by WA treatment (Figure 1A). This observation indicates that WA might activate the Nrf2 transcription factor pathway, leading to regulation of ARE-dependent genes. Since Nrf2 is involved in regulation of genes participating in heme degradation and glutathione biosynthesis pathways, the occurrence of the latter pathways in this IPA selected list might be a consequence of the primary effects of WA on regulation of the Nrf2 signaling (Figure 1B). In total 7 Nrf2 regulated genes were differentially regulated by WA, among which 6 were upregulated and 1 was down-regulated (Table 1). Differential expression of these genes induced by WA treatment was verified by qPCR analysis (Figure 1C). Among them the most prominently regulated gene was *HMOX1*, coding for HO-1 protein. It was the second strongest regulated gene in the top 10 list with about a 20-fold induction and statistically the most significantly differentially regulated gene upon treatment of HUVEC cells with WA.

3.2 Upregulation of HO-1 by WA in HUVECs and EA.hy926 endothelial cells

Based on the transcription profiling and qPCR verification data in HUVEC cells, we further characterized concentration- and time-dependent regulation of *HMOX1* by WA. qPCR analysis confirmed the increase of *HMOX1* mRNA level by WA treatment in a concentration- and time-dependent manner (figure 2A,B), correlating with increased HO-1 protein expression level (Figure 2C,D). After 6h of WA administration HO-1 protein levels reached a plateau phase upon which downregulation of HO-1 was observed (data not shown). Next, we compared *HMOX1* gene induction by WA with the effect of a structurally related withanolide WN and with the effect of DMSO, the vehicle in which WA and WN were solubilized. As expected, no increase in HO-1 expression could be observed by DMSO treatment and, remarkably, also not by the related withanolide. Similar results were obtained in the HUVEC-derived endothelial cell line EA.hy926 (Figure 2E-H). These results indicate that specifically WA, but not WN, induces HO-1 expression at the transcriptional and protein level in endothelial cells in a time- and concentration-dependent manner.

To confirm that the observed gene expression regulating effects are not due to WA-induced cytotoxicity, MTT assay was applied to define endothelial cell viability after exposure with different concentrations of WA for 24h. At concentrations up to 2µM, cells remained viable and no adverse effects on the growth of EA.hy926 and HUVEC cells could be observed (data not shown). These results confirm that the observed transcriptional regulatory effects by WA are not inherent or secondary to WA-induced cell death.

3.3 Role of Nrf2 in WA-induced upregulation of HO-1

To assess if activation of the transcription factor Nrf2 is implicated in WA-induced HO-1 upregulation, knockdown of Nrf2 was performed. Therefore, EA.hy926 cells were transiently transfected with Nrf2 siRNA and non-targeting siRNA as a control. Subsequently, Nrf2 and WA-induced HO-1 protein levels were analyzed by western blotting. Concomitantly with a clear downregulation of Nrf2 protein expression levels, induction of HO-1 expression by WA was also substantially decreased. In contrast, transfection of the non-targeting siRNA had no effect on expression levels of both proteins (Figure 3A), demonstrating the involvement of Nrf2 in WA-mediated HO-1 expression.

Previous studies demonstrated that upregulation of HO-1 by NRF2 can be mediated via binding of NRF2 to its antioxidant response element (ARE) consensus recognition sequence [34, 35]. Therefore we evaluated whether WA can regulate the expression of a luciferase reporter gene under control of this NRF2-regulated ARE-sequence in transiently transfected HEK293T cells. The transfected cells were either left untreated or were treated with different concentrations of WA. 6h WA treatment of HEK293T cells dose-dependently increased

luciferase expression levels (Figure 3B). As expected from results on the regulation of HO-1 expression, the WA related withanolide WN as well as the solvent control, i.e. DMSO, had no effect on ARE dependent luciferase expression. These results further strengthen the evidence that WA can regulate NRF2 dependent transcription.

3.4 Mechanism of action of WA induced NRF2 expression levels

Since activation of Nrf2 requires several sequential steps including inhibition of its continuous, proteasome-dependent degradation leading to its accumulation followed by nuclear translocation, the effect of WA on these different stages of the Nrf2 activation pathway was evaluated. An increase in the total endogenous expression level of Nrf2 by WA could be observed in EA.hy926 cells in a time-dependent manner, although not as prominent as by MG132, a direct inhibitor of the proteasome (Figure 4A). This time dependency perfectly correlates with the observed mRNA expression levels of HO-1. Further fractionation of the cellular lysates in cytoplasmic and nuclear fractions demonstrated that WA-mediated increase in Nrf2 protein expression levels results in increased nuclear translocation of Nrf2 (Figure 4B). These data confirm that WA can activate the transcription factor Nrf2 which then plays a key role in the HO-1 upregulation by WA in endothelial cells.

Altered Nrf2 protein levels can be obtained by changes in transcriptional or translation regulation or changes in protein stability. qPCR analysis on mRNA extracted from HUVEC cells treated with 1µM WA for 6h or left untreated revealed no effect of WA on Nrf2 mRNA transcript levels (Figure 4C). To further explore a possible effect of WA on Nrf2 protein stability, Ea.hy926 cells were pretreated with MG132 for 2h, resulting in increased Nrf2 protein levels. After vigorous washing of these cells to deplete MG132, cells were treated with CHX in the presence or absence of 1µM WA for different time points. Analyses of protein levels by western blot confirmed the short half-life of Nrf2, whose expression levels were hardly detectable after 90 minutes CHX treatment. In contrast, co-treatment with WA clearly prolonged Nrf2 stability up to 3h treatment, indicating that WA affects Nrf2 expression levels by inhibition of protein degradation (Figure 4D).

We next explored the molecular mechanism by which WA activates the NRF2 pathway. Since no effect of WA on the integrity of the Nrf2/KEAP1/Cul3 complex could be observed (data not shown), we evaluated whether WA affects Keap1-mediated ubiquitination of NRF2, as previously described for some NRF2 inducers [36-38]. Therefore a cell-based ubiquitination assay was performed in HEK293T cells transiently overexpressing NRF2, Keap1 and FLAG-tagged ubiquitin. The cells were either left untreated or were treated with different concentrations of WA (1 or 2µM) for 2h, along with the proteasome inhibitor MG132 (10µM). Addition of the latter allows the accumulation of ubiquitinated NRF2 leading to

comparable expression levels of NRF2 in all setups. As expected, co-expression of Keap1 with NRF2 significantly increased ubiquitination of NRF2. Interestingly, WA treatment markedly inhibited this ubiquitination of NRF2 already at 1µM concentration (Figure 4E).

3.4 Direct interaction of WA with Keap1

Based on the previous observations, it can be concluded that WA interferes with the Nrf2 activation pathway at an early step in the signaling cascade, taking place in the cytoplasm and influencing Nrf2 ubiquitination and consequently also stability. A major contribution to this step is provided by the Nrf2 negative regulator Keap1. Since Keap1 contains several redox-sensitive cysteine residues that can be modified leading to activation of Nrf2, we hypothesized that WA, being a thiol reactive compound, would inhibit Nrf2 ubiquitination by directly targeting Keap1. Via affinity purification using biotinylated WA (WA-BIOT), the potential binding of WA with Keap1 was investigated. Although the WA molecule was modified with a biotin moiety at its C27 position (Figure 5A), a residue which was suggested not to play a critical role in the biological activities of WA, we first evaluated the conservation of the bioactivity of this newly formed compound in the Nrf2 activation pathway in comparison with WA. Similarly to WA, WA-BIOT was able to induce HO-1 expression in endothelial cells indicating that the biotin modification did not alter the reactivity of the WA moiety in WA-BIOT (data not shown). Pull down analysis was performed by stimulating EA.hy926 cells with 1µM WA-BIOT for 2hours and capturing the WA-BIOT interacting proteins under stringent conditions using neutravidin beads. Interestingly, this affinity purification analysis demonstrated an interaction between WA-BIOT and Keap1 which could not be detected in the biotin-treated control cells (Figure 5B). Furthermore, higher molecular weight bands were observed upon treatment with WA-BIOT. This observation might indicate clustering of Keap1, however this hypothesis requires further analysis. Pretreatment with WA 1h before addition of WA-BIOT reduced the interaction of WA-BIOT with Keap1 indicating a competition of WA with WA-BIOT for binding to Keap1 and suggesting that the interaction of WA-BIOT with Keap1 occurs indeed via the WA moiety. Since DTT is a strong reducing agent affecting disulphide bonds, we hypothesized that co-treatment with DTT would reverse WA-Keap1 binding assuming that this binding is based on a Michael addition reaction of WA with cysteine residues in Keap1. As expected, under the condition of co-treatment with DTT, interaction between WA-BIOT and Keap1 was completely disrupted further strengthening the possibility of covalent linkage of WA with thiol groups in Keap1.

Since *in silico* modeling proposed that Nrf2 could also be a potential binding partner of WA [13], we investigated if WA-BIOT could also pull down Nrf2 and if the observed binding of WA-BIOT with Keap1 would be indirect via Nrf2. Thereto EA.hy926 cells were transfected with non-coding and Nrf2 siRNA. Using identical conditions as described above, we never

managed to detect an interaction of WA-BIOT with Nrf2 (Figure 5C). Furthermore, we were able to demonstrate that the interaction of WA-BIOT with Keap1 was not influenced by a strongly reduced expression level of Nrf2 (Figure 5C). These results indicate that in endothelial cells WA targets Keap1 independently of Nrf2 and that the cysteine residues within Keap1 might play an important role herein.

To further investigate if WA directly targets Keap1 and which site in Keap1 is involved in this interaction, recombinant Keap1 was incubated *in vitro* with WA. After trypsin digestion, peptide fragments bound to WA were analyzed by MALDI-TOF. As a negative control, a similar setup was included with the inactive withanolide WN instead of WA. Upon incubation with WA, several Keap1 trypsin fragments demonstrated altered m/z values correlating with covalent binding to WA (Figure 6A-B). These fragments all contained cysteine residues which, based on the reversion of interaction with DTT and on previous observations of Michael addition reaction by WA, are assumed as the WA target sites. Based on these observations Cys151, Cys319, Cys434, Cys489 and Cys613 are suggested to be involved in the interaction of Keap1 with WA. In contrast, no alterations were observed upon treatment with WN, correlating with the lack of effect of WN on the Nrf2 pathway.

These results indicate that WA can interact with different domains in Keap1. To confirm this observation in a cellular context we performed transient overexpression of either full length Keap1 or deletion mutants (ΔBTB, Δlinker and ΔKelch, lacking the BTB domain, the linker domain between BTB and Kelch domain, or the Kelch domain, respectively) (Figure 6D). The transfected cells were treated with WA-BIOT or biotin and after lysis and pull down interacting Keap1 proteins were evaluated by western blot using an antibody raised against the complete N-terminal end of Keap1. The obtained data confirm that WA can interact with all deletion mutants evaluated, so further confirming the *in vitro* data of multi-site targeting action of WA (Figure 6C). Furthermore higher order complexes were detected for all Keap1 variants evaluated, specifically upon WA-BIOT treatment. The identity of these complexes requires further investigation.

Analysis of the *in silico* models of Keap1 demonstrated that the potential WA interacting Cys residues are located at different sites of Keap1. Upon applying covalent docking software, which allows to integrate Michael addition reactions of WA with specific Keap1 Cys residues, lowest binding energy was observed for Cys319. Unfortunately predictions at this Cys, as well as Cys613, are less accurately predictable due to lack of crystal structures of the regions encompassing these residues. Almost comparable minimal binding energies and binding distances were obtained for interaction of WA with Cys151, Cys434, Cys489, which suggests potential redundant binding of WA to multiple Keap1 Cys residues (Figure 7).

4. Discussion

Withaferin A, one of the most bioactive molecules of the traditional Ayurvedic herb *Withania somnifera*, has demonstrated several biological activities including anti-inflammation, pro-apoptosis, anti-angiogenesis, etc. [2]. As such, WA holds promise for therapeutic applications of inflammatory diseases, cancer as well as neurologic disorders. However, high-quality insight in the effect of WA on different cell types is obligatory. Due to their strategic location, lining the blood vessels in a single continuous layer, endothelial cells play a crucial role in sensing various physiological and pathophysiological stressors as well as oxidative stress and xenobiotics. Therefore, we evaluated the effects of WA on endothelial cells to gain insight into WA-mediated transcription regulating effects.

In this paper, we demonstrated that WA strongly induces time- and concentration-dependently the expression of the antioxidant gene HO-1 in primary endothelial cells as well as in an endothelial cell line. The potential regulatory role of WA on HO-1 expression in endothelial cells has already been suggested by Bargagna-Mohan and colleagues, who demonstrated upregulation of HO-1 upon co-treatment of HUVEC cells with WA and VEGF or TNF [39]. In our study, we confirmed that this regulatory effect is mediated by WA alone. HO-1 is an important regulator of protection of cells against cytotoxicity or oxidative stress [40]. HO-1 catalyzes the first enzymatic step in the metabolism of free heme into ferrous iron, carbon monoxide (CO), and biliverdin, upon which biliverdin is subsequently converted to bilirubin by biliverdin reductase. Due to this decrease in heme levels and increase in biliverdin and bilirubin, HO-1 contributes to the repression of inflammation, including reduced polymorphonuclear leucocyte recruitment [41-45]. As a consequence regulation of HO-1 expression might have therapeutic implications, for instance, for treatment of vascular inflammatory diseases such as atherosclerosis. Indeed, some natural compounds have already been demonstrated to inhibit vascular inflammation by upregulation of HO-1 [46-48]. However by using knockdown of WA-induced HO-1 expression, we could not demonstrate an additive contribution of HO-1 regulation to the anti-inflammatory effects of WA (data not shown). Since the anti-inflammatory effect of HO-1 on endothelial cells was demonstrated to be mediated by downregulation of inflammation-induced expression of adhesion molecules [49], this result is not very surprising when we take into account the potent, direct inhibitory effects of WA on the pro-inflammatory NF-κB activation pathway [4].

HO-1 exhibits low basal expression levels in most cell types and becomes upregulated by a plethora of physiological and pathological stimuli including oxidative stress, cytokines, bacterial and electrophilic compounds. Several signal transduction pathways have been demonstrated to be involved in this process. These include activation of the mitogen activated protein kinases (MAPKs), activation of the phosphatidylinositol-3 kinase (PI3K)/Akt

pathway, activation of the JAK-STAT pathway [50-52]. Since JAK-STAT and Akt pathways are negatively affected by WA treatment either by inhibition of activation or by decreased protein stability [6, 53-55], rather opposing effects of WA on HO-1 expression could be expected. Effect of WA on MAPK activation has been mostly studied for p38. These studies demonstrated differential effects ranging from inhibitory to stimulatory effects, possibly cell type-dependent, but so far, to the best of our knowledge, endothelial cells have not been involved in these studies [8, 53, 56-58]. Instead, one of the most important master regulators in the transcriptional regulation of HO-1 expression is the transcription factor Nrf2, which binds as a dimer with small Maf proteins to antioxidant responsive elements (ARE) in the promoter region of HO-1 and many other stress-inducible antioxidant and phase II detoxifying genes [34, 50]. Recently, Vaishnavi and colleagues used molecular docking studies to demonstrate an interaction of WA and its related withanolide compound WN with the active site region of Nrf2. WA was suggested to bind to Nrf2 with higher affinity than WN [13]. However, using a biotinylated form of WA for *in vitro* detection of WA interaction partners, we were unable to demonstrate a direct interaction of WA with Nrf2. On the other hand, Vaishnavi and colleagues were unable to demonstrate an effect of WA on the Nrf2 activation pathway, as evaluated by analysis of Nrf2 expression levels and nuclear translocation in the human osteosarcoma cell line U2OS. In contrast, treatment of EA.hy926 cells with WA resulted in a time-dependent upregulation followed by increased nuclear translocation of Nrf2. These discrepancies might be the result of cell type-dependent activity of WA towards the Nrf2 activation pathway.

Under homeostatic conditions Nrf2 is kept inactive in the cytoplasm via its interaction with the inhibitor Keap1, which functions as an adaptor between Nrf2 and the ubiquitin ligase Cul3. The latter constitutively ubiquitinates Nrf2 leading to its proteasomal degradation [16, 59]. In the presence of electrophilic agents or oxidative stress, Nrf2 escapes from this control mechanism, becomes stabilized, accumulates and translocates to the nucleus. Based on the crucial role of Keap1 in this pathway as well as the knowledge that several natural compounds can activate the Nrf2 pathway by chemically reacting with Keap1, we evaluated this hypothesis for WA. Using the biotinylated form of WA, which exerts similar biological activities towards the regulation of HO-1 expression, we could confirm an interaction between WA and Keap1. This interaction is mediated by the WA moiety and probably involves thiol groups since it is hampered by pretreatment with WA or co-treatment with DTT, respectively. Unexpectedly, high molecular weight bands containing Keap1 could be observed upon treatment with biotinylated WA. Similar observations have previously been obtained by using other small electrophilic compounds [60, 61]. The composition of these bands remains however elusive and requires further investigation.

In human Keap1 27 Cys residues are present among which some have been identified to act as sensors of electrophilic and oxidative conditions. Several electrophilic compounds have been described to activate the Nrf2 pathway by exploiting these distinct reactive Keap1 cysteine residues [60, 62, 63]. For instance, Cys273 and Cys288 in the linker region showed an indispensable role in the suppression of Nrf2 by Keap1. Cys151 in the BTB domain (broad-complex, tramtrack and bric-a-brac domain) was described to be important in responsiveness to several Nrf2 inducers by its involvement in the interaction between Keap1 and the ubiquitin ligase Cul3 [21, 64]. As observed for most Keap1 targeting agents [65], also in case of WA different Cys target sides could be identified by proteomic mass spec analysis, in line with *in silico* predicted data. Thereby WA seem to evenly react through the total length of Keap1 attacking Cys151 in the BTB domain and 4 other sites located in the C-terminal Kelch domain, as previously described for the class of pure Michael acceptors [65]. This led us assume that the Nrf2 regulating activity of WA is probably mediated by multiple mechanisms on the Keap1-complex stability. Although no effect of WA on the Keap1-Cul3-NRF2 complex could be observed, a marked decrease of Keap1-mediated ubiquitination of NRF2 was observed. On the other hand, Keap1 has been demonstrated to act as an adaptor protein for the recruitment of additional target proteins to Cul3, besides Nrf2. These include the NF-κB activating kinase, IKKβ [66], as well as the anti-apoptotic protein, Bcl-2 [67], two proteins involved in key signal transduction pathways, which are strongly affected by WA [4, 68]. However, the observation that IKKβ and Bcl-2 protein expression levels were respectively unaltered or even reduced instead of increased by WA treatment (in analogy to Keap1 upregulation), suggests that WA targets more specifically the Keap1-Nrf2 pathway (unpublished results; [53, 56]).

Since oxidative stress is involved in various diseases involving immune and inflammatory responses, neurodegeneration, cardiovascular system, carcinogenesis and metastasis, increased antioxidant protection would be a strategy to prevent or treat the initiation or development of these disorders. One way to restore the oxidative imbalance is via activation of Nrf2. Several naturally occurring plant-derived compounds, such as curcumin from *Curcuma* and sulforaphane from *Broccoli*, have been demonstrated to activate Nrf2 [69, 70]. Some Nrf2 activating compounds have already been tested in animal models or even human clinical trials and were demonstrated to protect against moderate pulmonary hypertension, chronic kidney disease and multiple sclerosis [71-73]. Probably one of the best known Nrf2 activators is the dietary supplement Protandim®, also termed the Nrf2 synergizer, which by different laboratories was validated to activate Nrf2 and to reduce oxidative stress [71, 74, 75]. Interestingly, Ashwaganda extract is one of its ingredients suggesting that Nrf2 activation by Protandim® might be dependent on the presence of WA. To confirm the potential

therapeutic value of Nrf2 activation by WA additional studies are required to obtain better insight in the Nrf2 activating potential of WA in different physiological and pathological *in vitro* and *in vivo* conditions.

References

[1] Santagata S, Xu YM, Wijeratne EM, Kontnik R, Rooney C, Perley CC, et al. Using the Heat-Shock Response To Discover Anticancer Compounds that Target Protein Homeostasis. ACS Chem Biol 2011;7:340-9.

[2] Vanden Berghe W, Sabbe L, Kaileh M, Haegeman G, Heyninck K. Molecular insight in the multifunctional activities of Withaferin A. Biochem Pharmacol 2012;84:1282-91.

[3] Dave VP, Kaul D, Sharma Y, Bhattacharya R. Functional genomics of blood cellular LXR-alpha gene in human coronary heart disease. J Mol Cell Cardiol 2009;46:536-44.

[4] Kaileh M, Vanden Berghe W, Heyerick A, Horion J, Piette J, Libert C, et al. Withaferin a strongly elicits IkappaB kinase beta hyperphosphorylation concomitant with potent inhibition of its kinase activity. J Biol Chem 2007;282:4253-64.

[5] Koduru S, Kumar R, Srinivasan S, Evers MB, Damodaran C. Notch-1 inhibition by Withaferin-A: a therapeutic target against colon carcinogenesis. Mol Cancer Ther 2010;9:202-10.

[6] Lee J, Hahm ER, Singh SV. Withaferin A inhibits activation of signal transducer and activator of transcription 3 in human breast cancer cells. Carcinogenesis 2010;31:1991-8.

[7] Mehrotra A, Kaul D, Joshi K. LXR-alpha selectively reprogrammes cancer cells to enter into apoptosis. Mol Cell Biochem 2011;349:41-55.

[8] Min KJ, Choi K, Kwon TK. Withaferin A down-regulates lipopolysaccharide-induced cyclooxygenase-2 expression and PGE2 production through the inhibition of STAT1/3 activation in microglial cells. Int Immunopharmacol 2011;11:1137-42.

[9] Grover A, Shandilya A, Agrawal V, Pratik P, Bhasme D, Bisaria VS, et al. Blocking the chaperone kinome pathway: mechanistic insights into a novel dual inhibition approach for supra-additive suppression of malignant tumors. Biochem Biophys Res Commun 2010;404:498-503.

[10] Grover A, Shandilya A, Agrawal V, Pratik P, Bhasme D, Bisaria VS, et al. Hsp90/Cdc37 chaperone/co-chaperone complex, a novel junction anticancer target elucidated by the mode of action of herbal drug Withaferin A. BMC Bioinformatics 2011;12 Suppl 1:S30.

[11] Grover A, Shandilya A, Bisaria VS, Sundar D. Probing the anticancer mechanism of prospective herbal drug Withaferin A on mammals: a case study on human and bovine proteasomes. BMC Genomics 2010;11 Suppl 4:S15.

[12] Grover A, Shandilya A, Punetha A, Bisaria VS, Sundar D. Inhibition of the NEMO/IKKbeta association complex formation, a novel mechanism associated with the NF-kappaB activation suppression by Withania somnifera's key metabolite withaferin A. BMC Genomics 2010;11 Suppl 4:S25.

[13] Vaishnavi K, Saxena N, Shah N, Singh R, Manjunath K, Uthayakumar M, et al. Differential activities of the two closely related withanolides, Withaferin A and Withanone: bioinformatics and experimental evidences. PLoS One 2012;7:e44419.

[14] Itoh K, Chiba T, Takahashi S, Ishii T, Igarashi K, Katoh Y, et al. An Nrf2/small Maf heterodimer mediates the induction of phase II detoxifying enzyme genes through antioxidant response elements. Biochem Biophys Res Commun 1997;236:313-22.

[15] Lo SC, Li X, Henzl MT, Beamer LJ, Hannink M. Structure of the Keap1:Nrf2 interface provides mechanistic insight into Nrf2 signaling. EMBO J 2006;25:3605-17.

[16] Cullinan SB, Gordan JD, Jin J, Harper JW, Diehl JA. The Keap1-BTB protein is an adaptor that bridges Nrf2 to a Cul3-based E3 ligase: oxidative stress sensing by a Cul3-Keap1 ligase. Mol Cell Biol 2004;24:8477-86.

[17] Kobayashi A, Kang MI, Okawa H, Ohtsuji M, Zenke Y, Chiba T, et al. Oxidative stress sensor Keap1 functions as an adaptor for Cul3-based E3 ligase to regulate proteasomal degradation of Nrf2. Mol Cell Biol 2004;24:7130-9.

[18] Zhang DD, Lo SC, Cross JV, Templeton DJ, Hannink M. Keap1 is a redox-regulated substrate adaptor protein for a Cul3-dependent ubiquitin ligase complex. Mol Cell Biol 2004;24:10941-53.

[19] Katoh Y, Iida K, Kang MI, Kobayashi A, Mizukami M, Tong KI, et al. Evolutionary conserved N-terminal domain of Nrf2 is essential for the Keap1-mediated degradation of the protein by proteasome. Arch Biochem Biophys 2005;433:342-50.

[20] Magesh S, Chen Y, Hu L. Small molecule modulators of Keap1-Nrf2-ARE pathway as potential preventive and therapeutic agents. Med Res Rev 2012;32:687-726.

[21] Yamamoto T, Suzuki T, Kobayashi A, Wakabayashi J, Maher J, Motohashi H, et al. Physiological significance of reactive cysteine residues of Keap1 in determining Nrf2 activity. Mol Cell Biol 2008;28:2758-70.

[22] Taguchi K, Motohashi H, Yamamoto M. Molecular mechanisms of the Keap1-Nrf2 pathway in stress response and cancer evolution. Genes Cells 2011;16:123-40.

[23] Edgell CJ, McDonald CC, Graham JB. Permanent cell line expressing human factor VIII-related antigen established by hybridization. Proc Natl Acad Sci U S A 1983;80:3734-7.

[24] Dunning MJ, Smith ML, Ritchie ME, Tavare S. beadarray: R classes and methods for Illumina bead-based data. Bioinformatics 2007;23:2183-4.

[25] Heyninck K, Beyaert R. A novel link between Lck, Bak expression and chemosensitivity. Oncogene 2006;25:1693-5.

[26] Li X, Zhang D, Hannink M, Beamer LJ. Crystal structure of the Kelch domain of human Keap1. J Biol Chem 2004;279:54750-8.

[27] Tong KI, Padmanabhan B, Kobayashi A, Shang C, Hirotsu Y, Yokoyama S, et al. Different electrostatic potentials define ETGE and DLG motifs as hinge and latch in oxidative stress response. Mol Cell Biol 2007;27:7511-21.

[28] Zhuang C, Narayanapillai S, Zhang W, Sham YY, Xing C. Rapid identification of Keap1-Nrf2 small-molecule inhibitors through structure-based virtual screening and hit-based substructure search. J Med Chem 57:1121-6.

[29] Horer S, Reinert D, Ostmann K, Hoevels Y, Nar H. Crystal-contact engineering to obtain a crystal form of the Kelch domain of human Keap1 suitable for ligand-soaking experiments. Acta Crystallogr Sect F Struct Biol Cryst Commun 2013;69:592-6.

[30] Canning P, Cooper CD, Krojer T, Murray JW, Pike AC, Chaikuad A, et al. Structural basis for Cul3 protein assembly with the BTB-Kelch family of E3 ubiquitin ligases. J Biol Chem 2013;288:7803-14.

[31] Krieger E, Joo K, Lee J, Raman S, Thompson J, Tyka M, et al. Improving physical realism, stereochemistry, and side-chain accuracy in homology modeling: Four approaches that performed well in CASP8. Proteins 2009;77 Suppl 9:114-22.

[32] Ouyang X, Zhou S, Ge Z, Li R, Kwoh CK. CovalentDock Cloud: a web server for automated covalent docking. Nucleic Acids Res 2013;41:W329-32.

[33] Trott O, Olson AJ. AutoDock Vina: improving the speed and accuracy of docking with a new scoring function, efficient optimization, and multithreading. J Comput Chem 2010;31:455-61.

[34] Alam J, Stewart D, Touchard C, Boinapally S, Choi AM, Cook JL. Nrf2, a Cap'n'Collar transcription factor, regulates induction of the heme oxygenase-1 gene. J Biol Chem 1999;274:26071-8.

[35] Cho HY, Jedlicka AE, Reddy SP, Kensler TW, Yamamoto M, Zhang LY, et al. Role of NRF2 in protection against hyperoxic lung injury in mice. Am J Respir Cell Mol Biol 2002;26:175-82.

[36] Tao S, Rojo de la Vega M, Quijada H, Wondrak GT, Wang T, Garcia JG, et al. Bixin protects mice against ventilation-induced lung injury in an NRF2-dependent manner. Sci Rep 2016;6:18760.

[37] Tao S, Zheng Y, Lau A, Jaramillo MC, Chau BT, Lantz RC, et al. Tanshinone I activates the Nrf2-dependent antioxidant response and protects against As(III)-induced lung inflammation in vitro and in vivo. Antioxid Redox Signal 2013;19:1647-61.

[38] Wondrak GT, Villeneuve NF, Lamore SD, Bause AS, Jiang T, Zhang DD. The cinnamon-derived dietary factor cinnamic aldehyde activates the Nrf2-dependent antioxidant response in human epithelial colon cells. Molecules 2010;15:3338-55.

[39] Bargagna-Mohan P, Ravindranath PP, Mohan R. Small molecule anti-angiogenic probes of the ubiquitin proteasome pathway: potential application to choroidal neovascularization. Invest Ophthalmol Vis Sci 2006;47:4138-45.

[40] True AL, Olive M, Boehm M, San H, Westrick RJ, Raghavachari N, et al. Heme oxygenase-1 deficiency accelerates formation of arterial thrombosis through oxidative damage to the endothelium, which is rescued by inhaled carbon monoxide. Circ Res 2007;101:893-901.

[41] Hayashi S, Takamiya R, Yamaguchi T, Matsumoto K, Tojo SJ, Tamatani T, et al. Induction of heme oxygenase-1 suppresses venular leukocyte adhesion elicited by oxidative stress: role of bilirubin generated by the enzyme. Circ Res 1999;85:663-71.

[42] Kapturczak MH, Wasserfall C, Brusko T, Campbell-Thompson M, Ellis TM, Atkinson MA, et al. Heme oxygenase-1 modulates early inflammatory responses: evidence from the heme oxygenase-1-deficient mouse. Am J Pathol 2004;165:1045-53.

[43] Poss KD, Tonegawa S. Reduced stress defense in heme oxygenase 1-deficient cells. Proc Natl Acad Sci U S A 1997;94:10925-30.

[44] Willis D, Moore AR, Frederick R, Willoughby DA. Heme oxygenase: a novel target for the modulation of the inflammatory response. Nat Med 1996;2:87-90.

[45] Yachie A, Niida Y, Wada T, Igarashi N, Kaneda H, Toma T, et al. Oxidative stress causes enhanced endothelial cell injury in human heme oxygenase-1 deficiency. J Clin Invest 1999;103:129-35.

[46] Araujo JA, Zhang M, Yin F. Heme oxygenase-1, oxidation, inflammation, and atherosclerosis. Front Pharmacol 2012;3:119.

[47] Kim CK, Cho DH, Lee KS, Lee DK, Park CW, Kim WG, et al. Ginseng Berry Extract Prevents Atherogenesis via Anti-Inflammatory Action by Upregulating Phase II Gene Expression. Evid Based Complement Alternat Med 2012;2012:490301.

[48] Zhang SC, Shi Q, Feng YN, Fang J. Tissue-protective effect of glutamine on hepatic ischemia-reperfusion injury via induction of heme oxygenase-1. Pharmacology 2013;91:59-68.

[49] Soares MP, Seldon MP, Gregoire IP, Vassilevskaia T, Berberat PO, Yu J, et al. Heme oxygenase-1 modulates the expression of adhesion molecules associated with endothelial cell activation. J Immunol 2004;172:3553-63.

[50] Alam J, Cook JL. How many transcription factors does it take to turn on the heme oxygenase-1 gene? Am J Respir Cell Mol Biol 2007;36:166-74.

[51] Hamdulay SS, Wang B, Birdsey GM, Ali F, Dumont O, Evans PC, et al. Celecoxib activates PI-3K/Akt and mitochondrial redox signaling to enhance heme oxygenase-1-mediated anti-inflammatory activity in vascular endothelium. Free Radic Biol Med 2010;48:1013-23.

[52] Tron K, Samoylenko A, Musikowski G, Kobe F, Immenschuh S, Schaper F, et al. Regulation of rat heme oxygenase-1 expression by interleukin-6 via the Jak/STAT pathway in hepatocytes. J Hepatol 2006;45:72-80.

[53] Oh JH, Lee TJ, Kim SH, Choi YH, Lee SH, Lee JM, et al. Induction of apoptosis by withaferin A in human leukemia U937 cells through down-regulation of Akt phosphorylation. Apoptosis 2008;13:1494-504.

[54] Oh JH, Lee TJ, Park JW, Kwon TK. Withaferin A inhibits iNOS expression and nitric oxide production by Akt inactivation and down-regulating LPS-induced activity of NF-kappaB in RAW 264.7 cells. Eur J Pharmacol 2008;599:11-7.

[55] Um HJ, Min KJ, Kim DE, Kwon TK. Withaferin A inhibits JAK/STAT3 signaling and induces apoptosis of human renal carcinoma Caki cells. Biochem Biophys Res Commun 2012;427:24-9.

[56] Mandal C, Dutta A, Mallick A, Chandra S, Misra L, Sangwan RS. Withaferin A induces apoptosis by activating p38 mitogen-activated protein kinase signaling cascade in leukemic cells of lymphoid and myeloid origin through mitochondrial death cascade. Apoptosis 2008;13:1450-64.

[57] Yang ES, Choi MJ, Kim JH, Choi KS, Kwon TK. Combination of withaferin A and X-ray irradiation enhances apoptosis in U937 cells. Toxicol In Vitro 2011;25:1803-10.

[58] Zhang X, Mukerji R, Samadi AK, Cohen MS. Down-regulation of estrogen receptor-alpha and rearranged during transfection tyrosine kinase is associated with withaferin a-induced apoptosis in MCF-7 breast cancer cells. BMC Complement Altern Med 2011;11:84.

[59] Furukawa M, Xiong Y. BTB protein Keap1 targets antioxidant transcription factor Nrf2 for ubiquitination by the Cullin 3-Roc1 ligase. Mol Cell Biol 2005;25:162-71.

[60] Hong F, Freeman ML, Liebler DC. Identification of sensor cysteines in human Keap1 modified by the cancer chemopreventive agent sulforaphane. Chem Res Toxicol 2005;18:1917-26.

[61] Rachakonda G, Xiong Y, Sekhar KR, Stamer SL, Liebler DC, Freeman ML. Covalent modification at Cys151 dissociates the electrophile sensor Keap1 from the ubiquitin ligase CUL3. Chem Res Toxicol 2008;21:705-10.

[62] Kansanen E, Bonacci G, Schopfer FJ, Kuosmanen SM, Tong KI, Leinonen H, et al. Electrophilic nitro-fatty acids activate NRF2 by a KEAP1 cysteine 151-independent mechanism. J Biol Chem 2011;286:14019-27.

[63] Kobayashi M, Li L, Iwamoto N, Nakajima-Takagi Y, Kaneko H, Nakayama Y, et al. The antioxidant defense system Keap1-Nrf2 comprises a multiple sensing mechanism for responding to a wide range of chemical compounds. Mol Cell Biol 2009;29:493-502.

[64] He X, Ma Q. Critical cysteine residues of Kelch-like ECH-associated protein 1 in arsenic sensing and suppression of nuclear factor erythroid 2-related factor 2. J Pharmacol Exp Ther 2009;332:66-75.

[65] Holland R, Fishbein JC. Chemistry of the cysteine sensors in Kelch-like ECH-associated protein 1. Antioxid Redox Signal 2010;13:1749-61.

[66] Lee DF, Kuo HP, Liu M, Chou CK, Xia W, Du Y, et al. KEAP1 E3 ligase-mediated downregulation of NF-kappaB signaling by targeting IKKbeta. Mol Cell 2009;36:131-40.

[67] Niture SK, Jaiswal AK. INrf2 (Keap1) targets Bcl-2 degradation and controls cellular apoptosis. Cell Death Differ 2011;18:439-51.

[68] Mayola E, Gallerne C, Esposti DD, Martel C, Pervaiz S, Larue L, et al. Withaferin A induces apoptosis in human melanoma cells through generation of reactive oxygen species and down-regulation of Bcl-2. Apoptosis 2011;16:1014-27.

[69] Keum YS. Regulation of the Keap1/Nrf2 system by chemopreventive sulforaphane: implications of posttranslational modifications. Ann N Y Acad Sci 2011;1229:184-9.

[70] Shehzad A, Lee YS. Molecular mechanisms of curcumin action: signal transduction. Biofactors 2013;39:27-36.

[71] Bogaard HJ, Abe K, Vonk Noordegraaf A, Voelkel NF. The right ventricle under pressure: cellular and molecular mechanisms of right-heart failure in pulmonary hypertension. Chest 2009;135:794-804.

[72] Kappos L, Gold R, Miller DH, Macmanus DG, Havrdova E, Limmroth V, et al. Efficacy and safety of oral fumarate in patients with relapsing-remitting multiple sclerosis: a multicentre, randomised, double-blind, placebo-controlled phase IIb study. Lancet 2008;372:1463-72.

[73] Pergola PE, Krauth M, Huff JW, Ferguson DA, Ruiz S, Meyer CJ, et al. Effect of bardoxolone methyl on kidney function in patients with T2D and Stage 3b-4 CKD. Am J Nephrol 2009;33:469-76.

[74] Joddar B, Reen RK, Firstenberg MS, Varadharaj S, McCord JM, Zweier JL, et al. Protandim attenuates intimal hyperplasia in human saphenous veins cultured ex vivo via a catalase-dependent pathway. Free Radic Biol Med 2011;50:700-9.

[75] Qureshi MM, McClure WC, Arevalo NL, Rabon RE, Mohr B, Bose SK, et al. The Dietary Supplement Protandim Decreases Plasma Osteopontin and Improves Markers of Oxidative Stress in Muscular Dystrophy Mdx Mice. J Diet Suppl 2010;7:159-78.

The abbreviations used are: ARE, antioxidant response element; BTB, broad complex, tramtrack and bric-a-brac domain; CHX, cycloheximide; Cul3, Cullin-3; EpRE, electrophile response element; HO-1, heme oxygenase-1; HUVEC, human umbilical vein endothelial cells; Keap1, Kelch-like ECH associated protein 1; MALDI-TOF, matrix-assisted laser desorption/ionization time-of-flight tandem mass spectrometry; MAPK, mitogen-activated protein kinase; Nrf2, NF-E2-related factor 2; PI3K, phosphatidylinositol-3 kinase; TFA, trifluoroacetic acid; WA, Withaferin A; WA-BIOT, biotinylated Withaferin A; WN, Withanone

Conflict of interest

The authors declare no conflict of interest

Acknowledgements

This work has been supported by grants from Fonds voor Wetenschappelijk onderzoek-Vlaanderen (project 3G059713).

FIGURE LEGENDS

Figure 1. Pathway analysis of genes differentially regulated by WA in HUVEC cells.

(A) Top IPA pathways enriched with differentially expressed genes by WA. Top 17 most significantly affected pathways are presented. Fisher's exact test was used to calculate the p-value determining the probability that the associations between the genes in the data set and the canonical pathway is explained by chance. (B) Top IPA canonical pathways enriched with WA-regulated, differentially expressed genes. For each pathway percentage (upper panel) and number of genes being differentially up- or downregulated (lower panel) are presented. (C) qPCR analysis of the genes *HMOX1*, *HSPB8*, *DNAJB9*, *HERPUD1*, *GCLM*, *SQSTM1* and *ENC1*, genes influenced by WA and regulated by the Nrf2 pathway in HUVEC cells. Lower panel represents identical results without analysis of *HMOX1*. Values are normalized using PPIA reference gene. Statistical analysis was performed using Student's t-test (** $p<0.05$; *** $p<0.001$).

Figure 2. WA-mediated regulation of HO-1 expression in endothelial cells.

HUVEC (A-D) and EA.hy926 cells (E-H) were treated with 0.1µM, 0.5µM or 1µM WA, 1µM WN or DMSO as solvent control for 6h (A, C, E, G). Alternatively, the cells were treated with 1µM WA for 2h, 3h, 4h, 5h or 6h (B, D, F, H). *HMOX1* mRNA expression was analyzed by real-time quantitative PCR and normalized mRNA values relative to GAPDH levels were plotted (A, B, E, F). Effect of WA on HO-1 protein levels was evaluated by western blot with analysis of tubulin expression as loading control (C, D, G, H).

Figure 3. WA induces HO-1 expression via the transcription factor Nrf2.

(A) EA.hy926 cells were transiently transfected with non-targeting siRNA (control) or siRNA targeting specifically Nrf2. 24 hours after transfection cells were treated with 1µM WA for 6h upon which expression levels of Nrf2 and HO-1 were evaluated by western blot. Expression of tubulin was evaluated as a loading control. (B) HEK293T cells were transiently transfected with the ARE dependent luciferase reporter plasmid (pGL4.22-NQOI ARE-luc) and the β-galactosidase expression plasmid pUT651 for 24 h. The cells were treated with different concentrations of WA, 1µM WN or DMSO (concentration corresponding to highest concentration of WA) for 6 hours. Cells extracts were analyzed for luciferase activity and normalized for β-galactosidase activity. All values are expressed as mean values of six replicates.

Figure 4. Molecular mechanism of WA mediated NRF2 stabilisation

(A) EA.hy926 cells were treated with 1µM WA for different time points as indicated. MG132 and DMSO treatments function respectively as positive and negative control. Effect of WA on

Nrf2 expression level was then evaluated by western blot using anti-Nrf2 antibody. Expression of tubulin was evaluated as a loading control. (B) Cytoplasmic and nuclear proteins were isolated from EA.hy926 cells treated with 1µM WA for different time points. Expression levels of Nrf2 in these fractions were evaluated by western blot analysis using anti-Nrf2 antibody. To confirm correct cell fractionation presence of the cytoplasmic marker tubulin and the nuclear marker PARP in these fractions were analyzed by developing these blots with anti-tubulin and anti-PARP antibodies. (C) HUVEC cells were treated with 1µM WA or DMSO as solvent control for 6h. Nrf2 mRNA expression was analyzed by real-time quantitative PCR and normalized mRNA values relative to cyclophilin levels were plotted. (D) EA.hy926 cells were left untreated or were pretreated with 10µM MG132 for 2 hours after which cells were washed and treated with 10µg/ml CHX either in presence or absence of 1µM WA. At different incubation times, cells were lysed and protein levels were evaluated by western blot using Nrf2 specific antibody. Expression of tubulin was evaluated as a loading control. (E) WA affects Keap1-mediated ubiquitination of NRF2. HEK293T cells were transiently transfected with expression vectors encoding HA-tagged NRF2, FLAG-tagged ubiquitin and Keap1. 24 hours after transfection cells were stimulated with 1 or 2µM WA or left untreated for 2h. 1,5 hour before lysis all setups were treated with 10µM MG132 to equalize NRF2 expression levels in all setups. Anti-NRF2 immunoprecipitates (IP) were analyzed by immunoblotting with anti-FLAG antibody for detection of ubiquitinated NRF2. Total lysates (input) were evaluated for overexpression of NRF2 and Keap1 by western blotting using anti-NRF2 and anti-Keap1 antibodies.

Figure 5. WA binds to Keap1 independent of Nrf2.

(A) Structure of WA and biotinylated WA (WA-BIOT). (B) EA.hy926 cells were treated for 2 hours with 1µM biotinylated WA or 1µM biotin (-). When indicated 1 hour pretreatment with WA (2µM) or DTT (1µM) as controls was performed. After lysis of the cells interacting proteins were affinity purified using neutravidin beads. Western blot analysis on total lysate (input) and affinity purified proteins were performed using anti-Keap1 polyclonal antibodies. (C) EA.hy926 cells were transfected with Nrf2 specific siRNA or non-targeting siRNA. 24h after transfection cells were treated with 1µM WA-BIOT or 1µM biotin for 2 hours. Cells were lysed and WA-BIOT interacting proteins were purified using neutravidin beads. Expression levels of endogenous Nrf2 and Keap1 in total cell lysates and pull down lysates were evaluated by western blot analysis using specific anti-Nrf2 (upper panel) and Keap1 (lower panel) antibodies (HMW: high molecular weight bands).

Figure 6. Structural analysis of interaction of WA with Keap1

(A) MALDI-TOF analysis of isolated Keap1 (0.1 mg/ml) incubated with 50 µM WA or 50 µM

WN, as negative control, incubated for 30 min at 37˚C. After digestion with trypsin the mass spectrum of Keap1 was measured. The spectrum of Keap1 incubated with control solvent displayed no peak at m/z 2604.7 (upper panel). The incubation with WA showed a peak with m/z 2604.7, which corresponds to the mass of the adduct of WA (470.6 dalton) on the peptide with mass m/z 2134.1 (middle panel). The amino acid sequence of the peptide is CVLHVMNGAVMYQIDSVVR, which contains Cys151. The spectrum of Keap1 incubated with WN did not show a peak at m/z 2604.7 (lower panel). (B) The incubation with WA (middle panel of each peptide spectrum) also showed extra peaks with m/z 2512.7, 3254.2, 1815.2, 1904.3 which correspond to the masses of the adducts of WA on the peptides IFEELTLHKPTQVMPCR (m/z 2042.1), IGVGVIDGHIYAVGGSHGCIHHNSVER m/z 2783.6), LNSAECYYPER 1344.5 (m/z), SGVGVAVTMEPCRK 1433.7 (m/z), which contain Cys 319, 434, 489, 613, respectively (spectra from left to right). (C) HEK293T cells were transiently transfected with different Keap1 full length or deletion mutants encoding plasmids, as indicated. 24 hours after transfection cells were treated with biotin or WA-BIOT for 2h. After lysis of the cells interacting proteins were affinity purified using neutravidin beads. Western blot analysis on total lysate (input) and affinity purified proteins were performed using anti-Keap1 N-terminus polyclonal antibodies. (D) Linear representation of human Keap1 sequence with indication of 27 Cys residues and the principal BTB and Kelch domains. The 5 Cys residues identified as WA target sites are indicated in boxes.

Figure 7. *In silico* modeling of interaction of WA with Keap1

(A) For the 5 Cys WA target residues the binding energy and distance of the covalent bond with WA as predicted by covalent docking method based on the indicated crystal structures are indicated (NA: crystal structure not available) (B) Docking analysis of WA on Cys151 located in the BTB domain as determined by the crystal structure 4CXI. (C) Docking analysis of WA on Cys 489 located in the Kelch domain as determined by the crystal structure 4IFL.

Table 1: List of significantly, differentially expressed genes, with at least 2-fold change down- or upregulation by WA-treatment of HUVEC cells. (FC: fold change; IF: induction factor). NRF2-regulated genes are indicated in bold.

genes	Log2FC	IF	p-value
HSPA1A	4.5	22.24	2.9E-05
HMOX1	**4.4**	**20.94**	**4.3E-07**
HSPA1B	3.6	12.12	2.7E-05
OSGIN1	2.9	7.52	1.2E-05
DNAJB1	2.4	5.38	4.9E-04
ZFAND2A	2.3	5.04	6.1E-04
MIR22HG	2.0	4.01	4.0E-06
OSGIN1	1.9	3.72	4.9E-05
KLF2	1.8	3.58	4.9E-04
ZFP36	1.8	3.50	1.0E-03
SLC2A3	1.6	3.03	1.0E-04
BAG3	1.6	3.03	2.9E-03
DEDD2	1.6	2.98	3.2E-03
HSPB8	**1.5**	**2.87**	**1.1E-03**
HSPH1	1.5	2.84	3.2E-03
DUSP1	1.5	2.74	3.6E-03
DNAJB9	**1.4**	**2.70**	**1.7E-03**
IL8	1.4	2.69	3.0E-02
HERPUD1	**1.4**	**2.63**	**1.0E-02**
DDIT3	1.4	2.63	2.8E-02
GCLM	**1.3**	**2.53**	**5.3E-05**
SRXN1	1.3	2.50	5.9E-04
SLC3A2	1.3	2.41	1.2E-02
CHORDC1	1.2	2.35	1.6E-02
INSIG1	1.2	2.33	1.3E-03
SLC7A5	1.2	2.27	2.3E-02
CD55	1.2	2.26	1.1E-03
BANP	1.2	2.25	1.2E-03
ULBP2	1.2	2.24	1.3E-04
PPP1R15A	1.2	2.22	4.0E-03
IL8	1.1	2.21	6.8E-02
AGPAT9	1.1	2.20	6.3E-04
UGDH	1.1	2.20	3.5E-05
HERPUD1	1.1	2.17	2.0E-02
DUSP5	1.1	2.16	5.6E-02
CDC42EP2	1.1	2.15	1.5E-02
LDLR	1.1	2.14	3.9E-03
SERTAD1	1.1	2.12	1.5E-03
SAT1	1.1	2.12	7.4E-02
RIT1	1.1	2.12	8.3E-03
SQSTM1	**1.1**	**2.08**	**9.6E-04**
MEG3	1.0	2.06	5.2E-02
HSPA8	1.0	2.05	6.7E-04
P4HA2	1.0	2.02	8.0E-02
NPC1	1.0	2.01	3.5E-02
MYCT1	1.0	2.00	2.5E-03
FJX1	-1.0	0.48	1.7E-03
THBS1	-1.0	0.49	3.1E-02
SERTAD4	-1.0	0.49	4.7E-04
ENC1	**-1.0**	**0.49**	**1.1E-03**
MTUS1	-1.0	0.49	1.1E-02
IMP3	-1.0	0.49	5.6E-06

EDN1	-2.4	0.50	1.1E-02

Figure

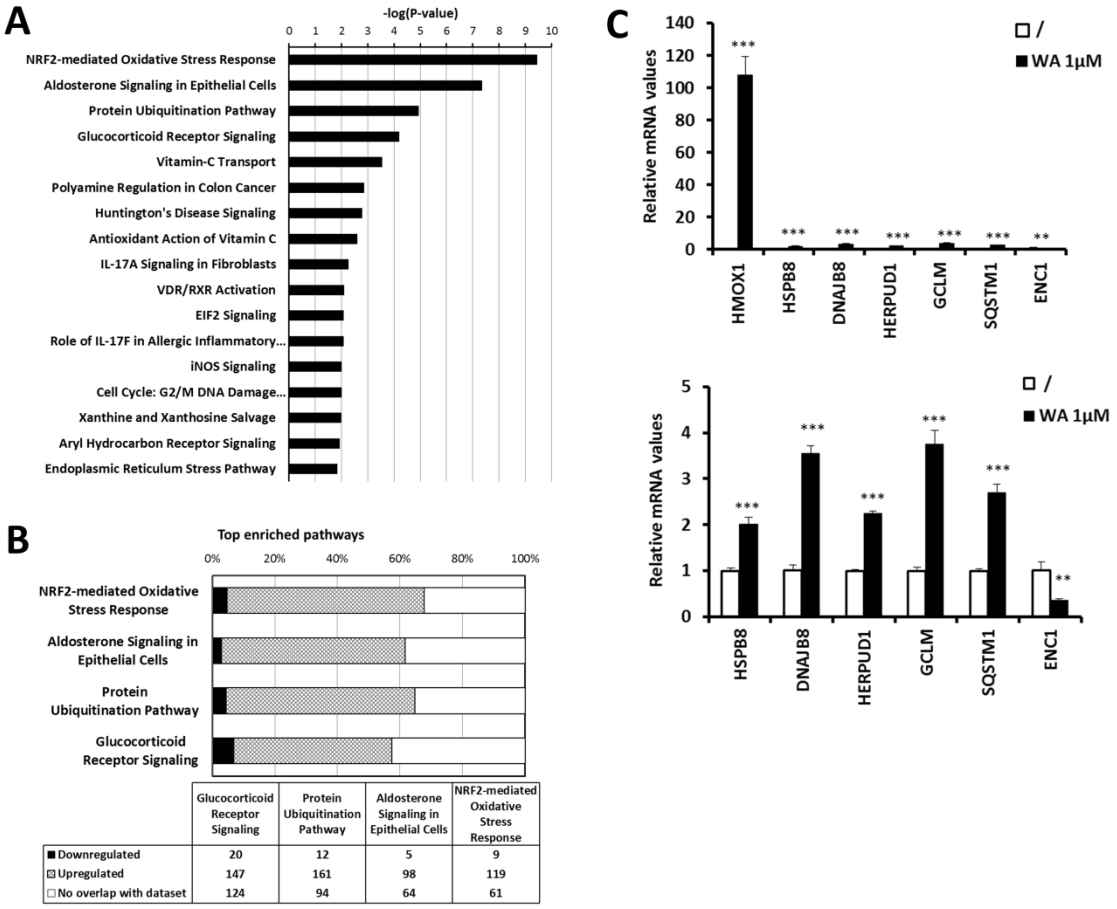

Heyninck et al., Figure 1

Figure

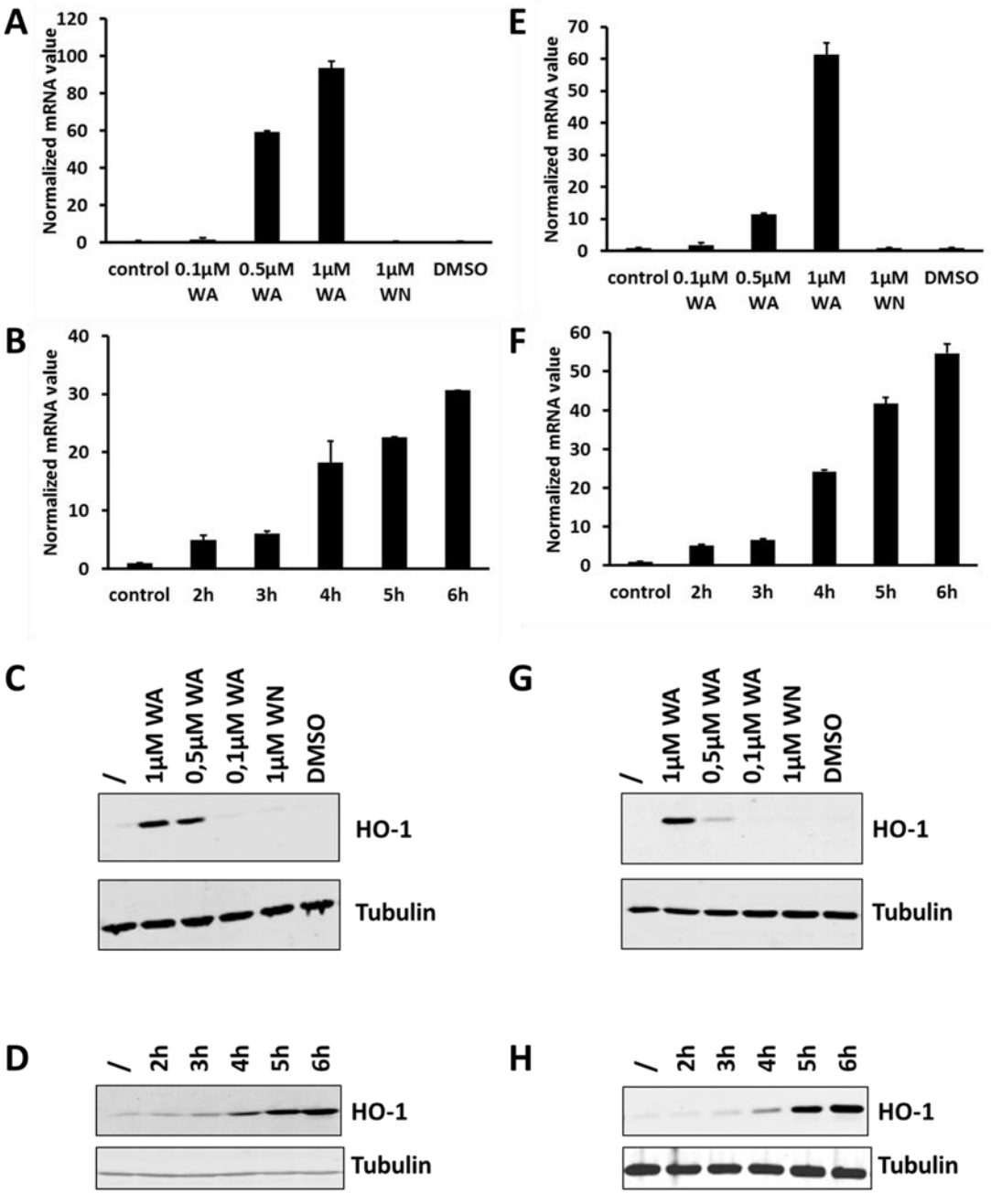

Heyninck et al., Figure 2

Figure

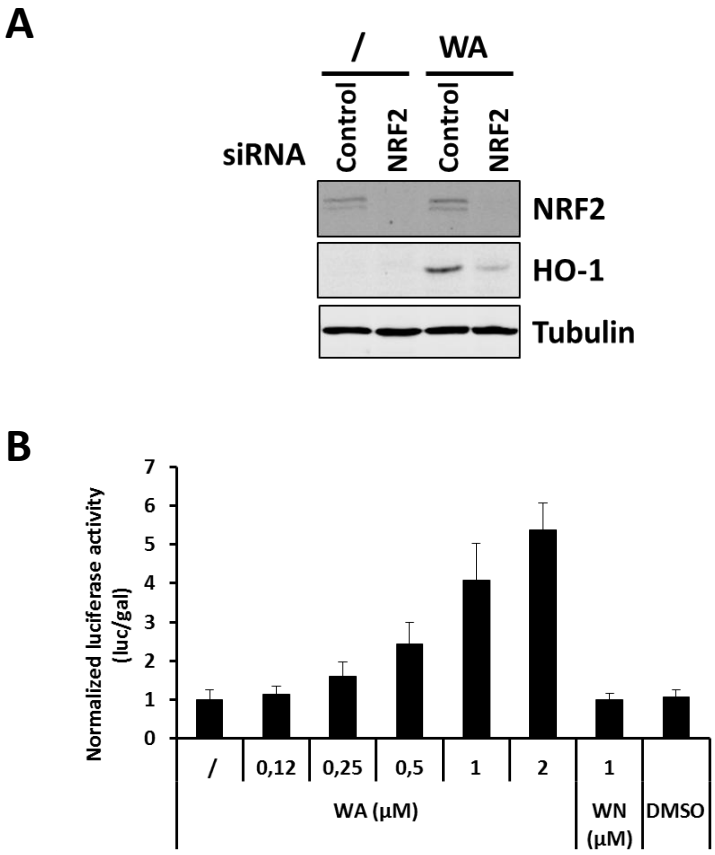

Heyninck et al., Figure 3

Figure

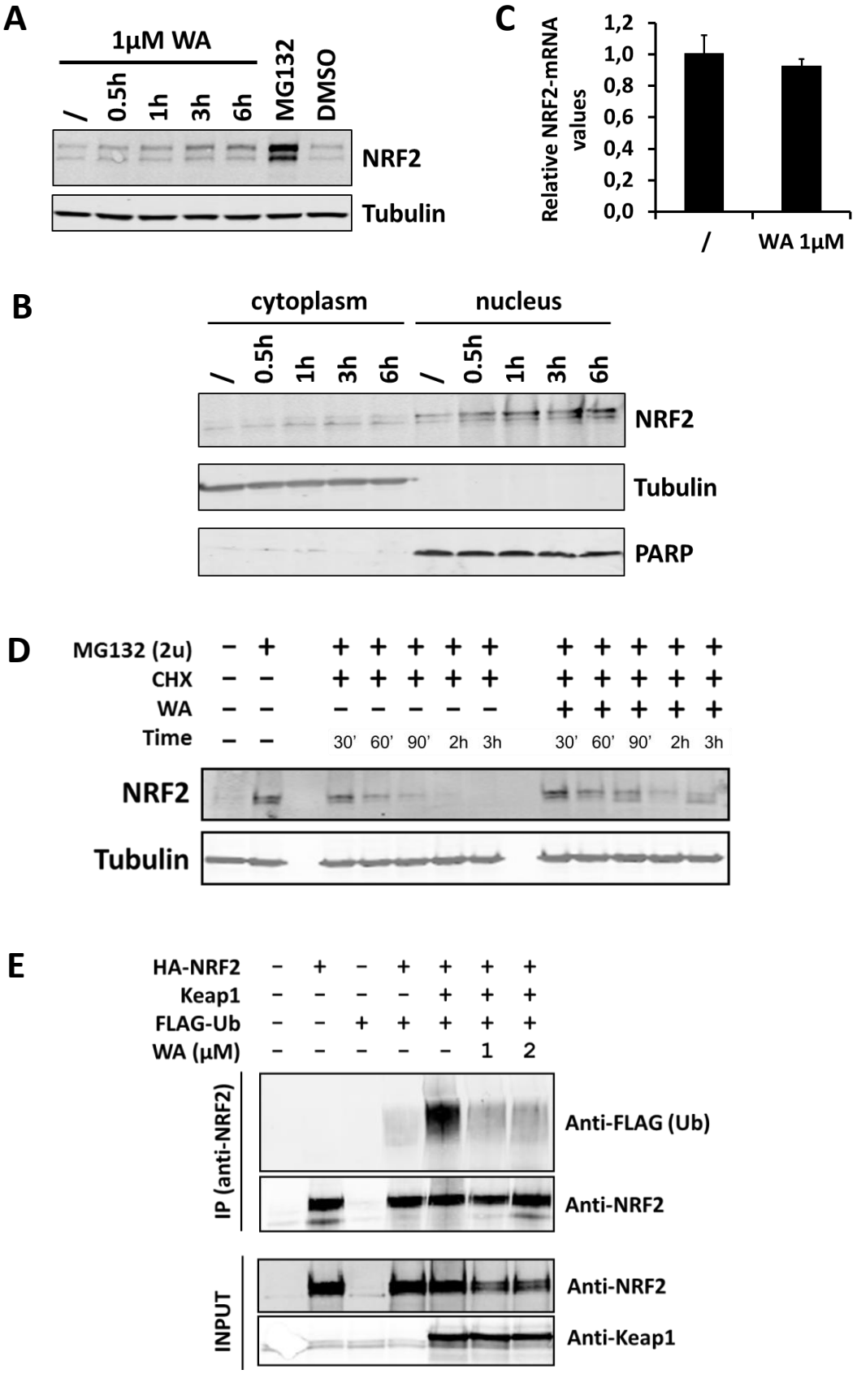

Heyninck et al., Figure 4

Figure

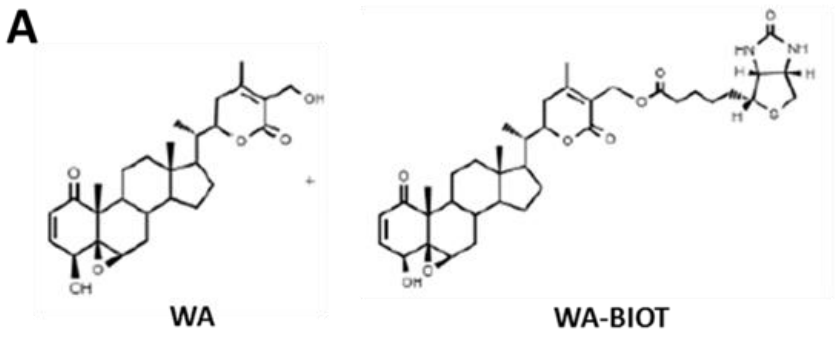

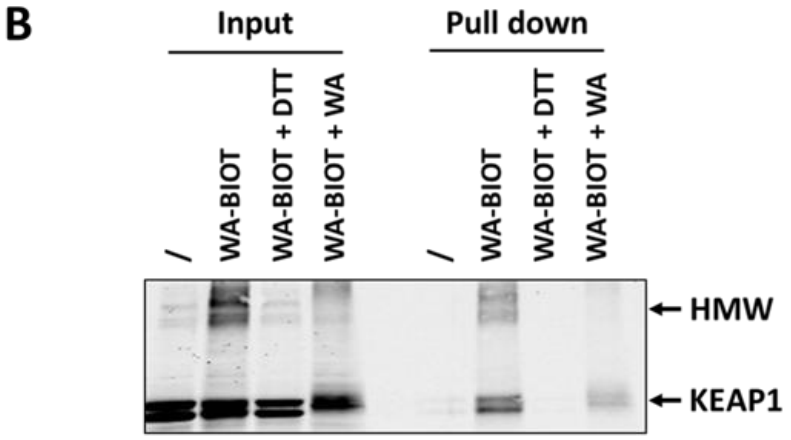

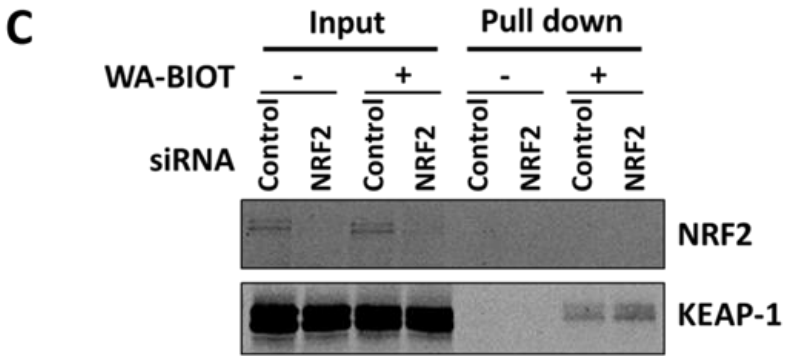

Heyninck et al., Figure 5

Figure

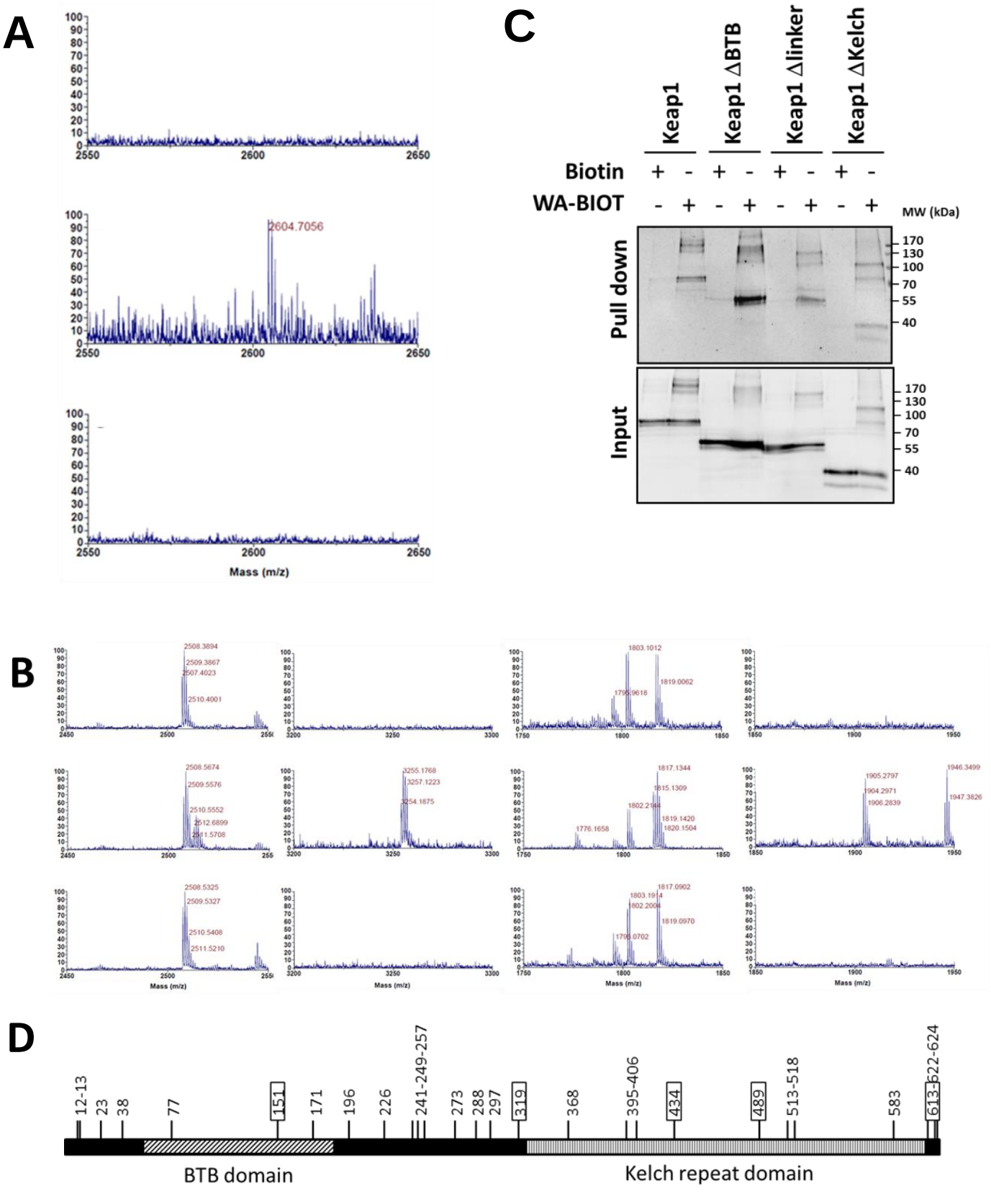

Heyninck et al., Figure 6

Figure

A

Keap1 interaction site	PBD crystal structure	Estimated G (Kcal/mole)	Bond length (Angstrom Units)
Cys 151	4CXI BTB domain	-10.16	1.85
Cys 319	NA	-11.05	1.86
Cys 434	4IFL Kelch domain	-9.40	1.89
Cys 489	4IFL Kelch domain	-9.54	1.90
Cys 613	NA	-9.36	1.86

B

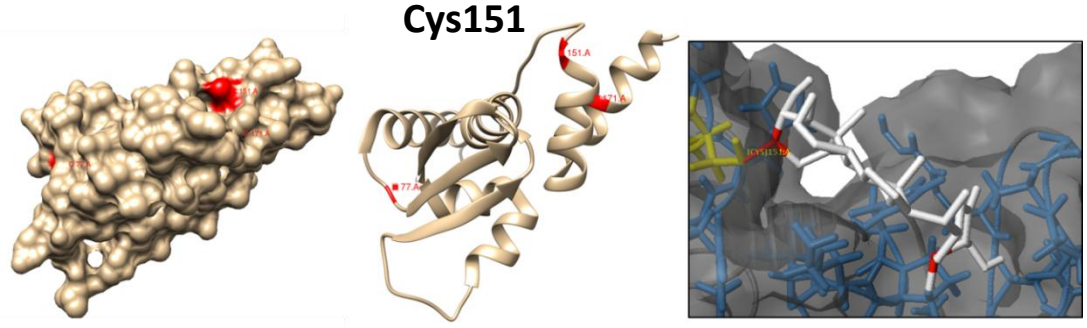

C

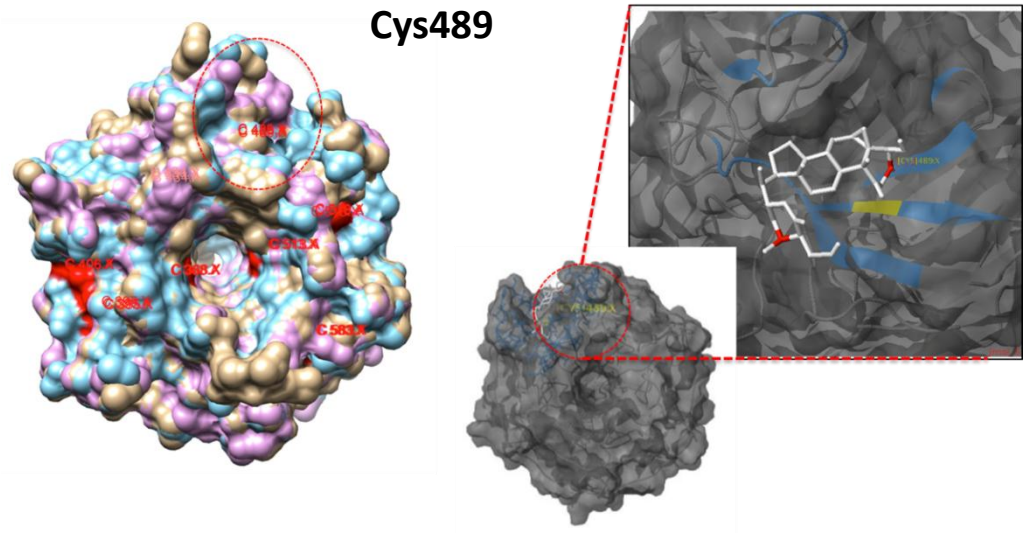

Heyninck et al., Figure 7